



## PAPER

## Investigation of tribological behavior of 20NiCrBSi-WC12Co coated brake disc by HVOF method

## OPEN ACCESS

## RECEIVED

31 October 2019

## REVISED

10 December 2019

## ACCEPTED FOR PUBLICATION


13 December 2019

## PUBLISHED

13 January 2020

Original content from this work may be used under the terms of the [Creative Commons Attribution 4.0 licence](#).

Any further distribution of this work must maintain attribution to the author(s) and the title of the work, journal citation and DOI.

Halil Kılıç<sup>1,3</sup>  and Cenk Mısırlı<sup>2</sup><sup>1</sup> Kırklareli University, Technical Sciences Vocational School, Kırklareli, Turkey<sup>2</sup> Trakya University, Faculty of Engineering, Edirne, Turkey<sup>3</sup> Author to whom any correspondence should be addressed.E-mail: [halil.kilic@klu.edu.tr](mailto:halil.kilic@klu.edu.tr) and [cenkm@trakya.edu.tr](mailto:cenkm@trakya.edu.tr)

Keywords: brake disc testing, coating, tribological behavior, wear rate, HVOF spraying

**Abstract**

In braking systems, which consist of dry sliding lining against a pearlitic cast-iron disc, disc wear has a significant impact on the overall wear rate. In this work, dynamometer tests were conducted to find out the friction and wear behaviour of 20NiCrBSi-WC12Co cermet coating accumulated on the cast-iron disc by High velocity oxy-fuel spraying (HVOF) and the findings were compared with those of the uncoated disc. Braking tests of the coated and uncoated discs were performed on a full-scale brake dynamometer, which was designed in line with the SAE-J2430 Brake Effectiveness Procedure. Microhardness values, surface properties, scanning electron microscopy (SEM) analysis, energy dispersive x-ray (EDX) and x-ray diffraction (XRD) analysis of the discs were evaluated. As a result of these analyses, it was found out that cermet coating had a much higher microhardness and abrasion resistance with the combination of hard WC phase and mild Ni matrix compared to the conventional disc. The coated disc exhibited stable braking effectiveness with lower surface contact temperature. At the same time, this coating results in longer service life by reducing abrasive wear on the brake disc surface and a lower lining wear rate, reducing particle matter emissions to the environment.

**1. Introduction**

The brake disc and linings, must meet the requirements of good wear resistance [1], stable coefficient of friction [2], reduced noise and reduced particle matter emissions [3, 4]. To meet these requirements, the temperature formed by the correct thermal conductivity and friction layer formation conditions are often referred to as key features [5–7] and is therefore covered by many studies [8, 9].

The tribological behaviour of the brake friction materials is controlled by the properties of the friction layer formed on the lining and disc contact surface. The performance of the system is very sensitive to the contact temperature [10, 11]. The coefficient of friction is relatively high, but most importantly it must be stable. In addition to the safety requirements, there are requirements such as long life and high comfort [12]. The nature of the brake system differs significantly from many other tribological contact cases. This tribological contact includes dry sliding contact at high speeds, high contact forces and high temperatures. The disc lining pair experiences dry sliding contact for about 50% of the braking time. Therefore, the properties of organic and inorganic compounds deteriorate at high contact temperatures, the coefficient of friction decreases and the wear rate increases. The studies in the relevant literature have revealed that wear residues from friction materials make up a significant proportion of particle emissions to the environment [13] and that these particles are often below 20  $\mu\text{m}$  [13, 14]. An ideal brake system should provide a stable friction behaviour under all operating conditions [15]. High power densities cause high surface temperatures and therefore bring special demands for friction materials. It is of interest to consider thermal spray cermet coatings as an alternative to these materials [16–18].

Thermal spraying is an important technique in improving the surface properties of materials. High velocity oxy-fuel spraying (HVOF) is one of the most commonly used techniques and can be applied to a wide range of materials. The HVOF method prevents decarburization with its superior properties such as high flame speed

and low flame temperature, reducing the formation of harmful reaction products. Typical HVOF coatings have a hardness in the 900–1200 HV range depending on the carbide type and metal matrix. With high spray speeds (up to  $500 \text{ m s}^{-1}$ ), coatings with low porosity and high abrasion resistance can be cumulated [19]. Therefore, it is considered to be one of the most suitable methods for the preparation of cermet coatings [20].

WC-based coatings are generally used where erosion and abrasion resistance is demanded. Because of the unique combination of high and medium hardness, WCCo coatings exhibit high resistance to various types of wear, such as sliding, erosion and wear [21]. Ni-based NiCrBSi coatings are widely used in high temperature, corrosion and wear resistance applications [22]. Hardness and wear properties can be improved by adding different powder properties into NiCrBSi coating powder. With the addition of WC into NiCrBSi, one of these powders, high microhardness, high abrasion and corrosion resistance has been achieved which is the reason why it has attracted attention of so many researchers [23–25]. Nickel in the powder components of 20NiCrBSi-WC12Co exhibits a good adhesion with its excellent wettability, and improves Chrome tribo-mechanical properties. Boron reduces the melting temperature and contributes to the formation of hard phases. Silicon increases the viscosity while lowering the melting temperature. Iron, while regulating the diffusion rate, increases the hardness and wear resistance by providing the formation of carbon-hard carbides. Tungsten carbide provides high abrasion resistance [26]. Cobalt acts as a binder to form a ductile, dense and well-adhered tribofilm on the surface to protect the surface from wear. Usually using Co and Cr as binders significantly improves the sliding/wear resistance of the coating compared to  $\text{Cr}_2\text{C}_3$  [27]. In the dry sliding tests of HVOF cermet coatings, steel or ceramic materials were generally used as counter surfaces. Research has revealed that only a few studies using brake friction material as the counter surface [19, 28]. It is understood that the amount of wear and brake performance of the commercial brake discs are the factors that need further investigation.

In this study, the braking performance of 20NiCrBSi-WC12Co coated brake disc through HVOF method was investigated. Experimental tests of the coated and uncoated brake discs were carried out on a brake tester designed in line with the J2430 [29] test procedure recommended by SAE (Society of Automotive Engineers). Braking test results of the discs, microhardness values, microstructure analysis, wear amounts and lining surface properties were evaluated together. The study aimed to determine the braking characteristics of the HVOF cermet coating against the commercial brake lining and to evaluate the effect of this coating on the friction and wear performance of the disc-lining pair.

## 2. Experimental

### 2.1. Braking pairs

The cast-iron discs of OEM, which is an original equipment producer, were used in the braking tests. Figure 1(a) shows the microstructure of typical grey iron-containing free ferrite with a pearlitic matrix between graphite liners. Figure 1(b) shows the EDX mapping analysis of cast iron. Here, the distribution of elements in the area corresponding to the SEM image of the cast iron has been determined by EDX analysis and indicated by the area color scale. The discs have 280 mm diameter, 140 mm inner diameter, 100 mm hub diameter, 24 mm thickness, 44 mm height. Besides, it has air cooling channels and has standard surface properties. The composition of the commercial brake disc used in the tests is shown in table 1. In the experimental studies, commercial brake linings of the same formulation were used as the friction material. As a result of the tests, it was determined that the lining had a high density of approximately  $2.5 \text{ g cm}^{-3}$ . The brake linings have been prepared under the SAE-J661 [30] Brake Lining Quality Control Test Procedure with a surface area of  $\text{inch}^2$  and a thickness of approximately 12 mm as shown in figure 2.

### 2.2. Characterization of coating powder

Commercially available 20NiCrBSi-WC12Co spray powder was used to form the coating system. Coating powder (Cr:17, B:3.5, Si:4, C:1, Fe:4, Ni:bal., Co: <13.5, C: <5.8, Fe: <0.2, W:bal.; wt%) is in 15–53  $\mu\text{m}$  grain size, produced in globe-type and blended form. These materials consist of a self-flowing alloy which is blended with a hard phase of tungsten carbide in a cobalt or nickel matrix. As a result of the laser diffraction analysis, the particle size distribution graph of the coating powder between 12–45  $\mu\text{m}$  was obtained as shown in figure 3. Figure 4 shows the typical shape and size of both powders: spherical morphology NiCrBSi metallic alloy and other particles are WC12Co.

### 2.3. HVOF spray process

In the spray coating system, JP5000 Tafa-Praxair HVOF spray gun was used. To increase the bonding strength of the coating on the brake disc, the surfaces of the disc were cleaned and dried with hot air and roughened by sandblasting corundum grit ( $\text{Al}_2\text{O}_3$ , 30/50 mesh) with Ra: 10–12  $\mu\text{m}$  for 10 min at 5 bar pressure. The coating process was immediately started to prevent the disc and coating layer interface from being affected by

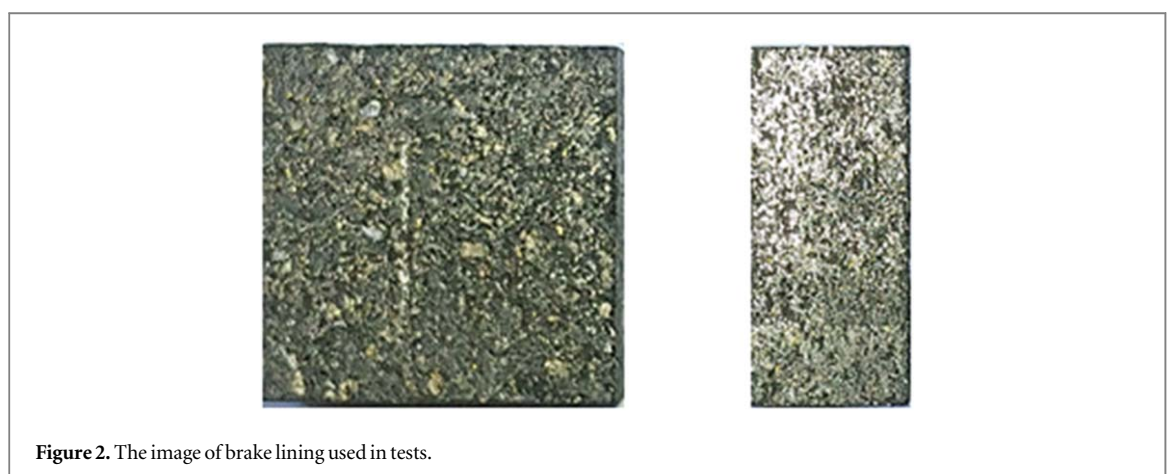
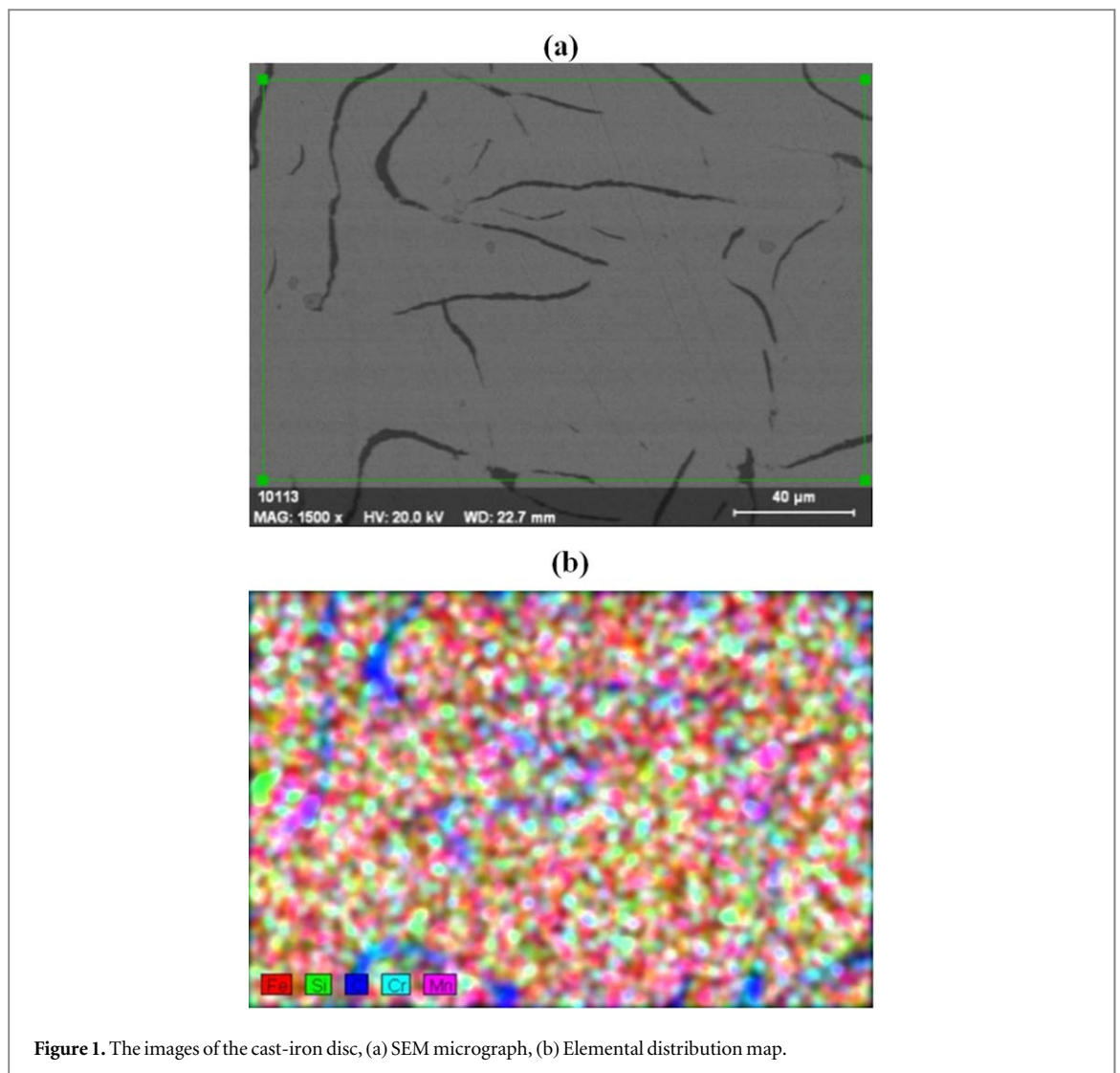


**Table 1.** Composition of the cast-iron disc (wt%).

C	Si	Mn	Cr	P	S	Fe
3.4	1.88	0.54	0.12	0.181	0.066	Balance

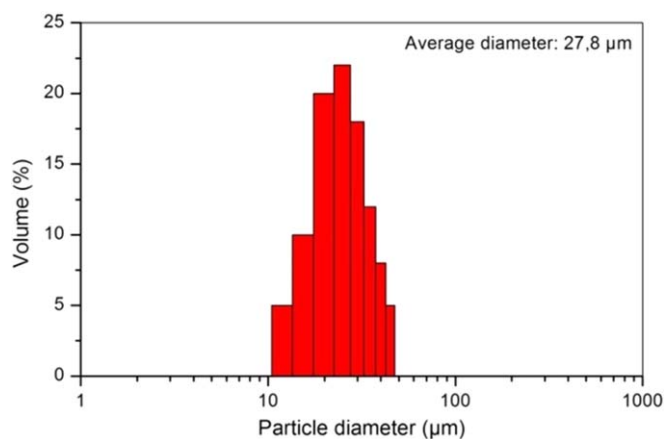


Figure 3. The particle size distribution of coating powder sample.

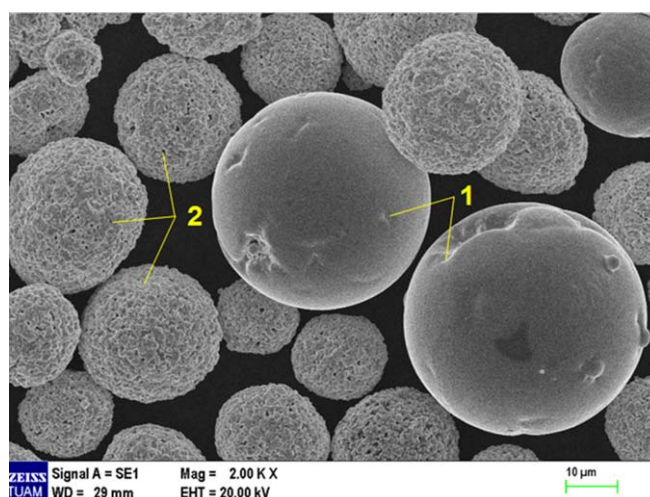


Figure 4. Powder morphology 1-NiCrBSi, 2-WC12Co.

Table 2. HVOF process parameters.

Parameters	JP-5000
Kerosene flow rate ( $\text{l min}^{-1}$ )	0.416
Oxygen flow rate ( $\text{m}^3 \text{h}^{-1}$ )	54
Backside cooling (bar)	3–5
Powder flow ( $\text{g min}^{-1}$ )	75
Disk revolution speed (rpm)	130
Barrel length (mm)	200
Spray distance (mm)	330
Powders size ( $\mu\text{m}$ )	12–45
Layer thickness per pass ( $\mu\text{m}$ )	15–20
Coating thickness ( $\mu\text{m}$ )	370

atmospheric oxidation. To prevent overheating of the brake disc during thermal spraying, cooling is carried out with compressed air after coating the surface. Spray parameters and final coating thickness are listed in table 2.

#### 2.4. Braking test procedure

To determine the braking performance of the discs, laboratory scale dynamometer tests were performed. The tests used original equipment brake calipers and commercial brake linings. A schematic diagram of the dynamometer used in the test is shown in figure 5. The test instrument is a full-scale dynamometer which meets

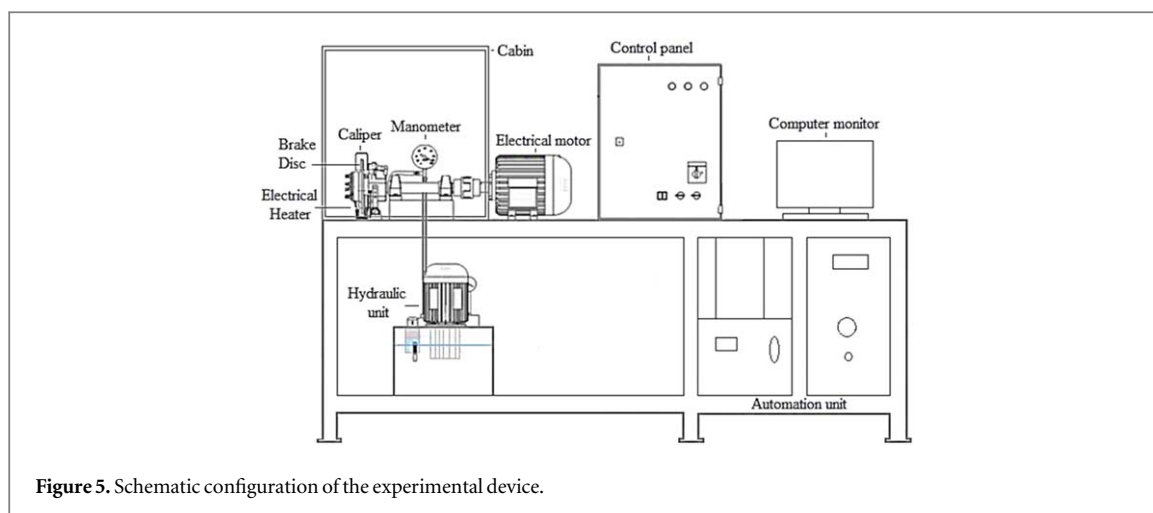


Figure 5. Schematic configuration of the experimental device.

Table 3. Test conditions of SAE-J2430.

Section	Test name	Conditions
1	Instrument check stop	50 → 3 km h <sup>-1</sup> ; 10 bar; 5 stops 100 → 3 km h <sup>-1</sup> ; 10 bar; 5 stops 50 → 3 km h <sup>-1</sup> ; 7–14 bar; 8 stops 100 → 3 km h <sup>-1</sup> ; 16 bar; 5 stops
2	Burnish	80 → 3 km h <sup>-1</sup> ; 8 bar; 200 stops
3	Effectiveness	50 → 3 km h <sup>-1</sup> ; 12 bar; 5 stops 100 → 3 km h <sup>-1</sup> ; 14–16 bar; 11 stops
4	Fade	120 → 56 km h <sup>-1</sup> ; 10–14 bar; 15 stops
5	Hot performance	100 → 3 km h <sup>-1</sup> ; 10–18 bar; 2 stops
6	Cooling	50 → 3 km h <sup>-1</sup> ; 13–10 bar; 4 stops
7	Recovery ramp	100 → 3 km h <sup>-1</sup> ; 12–10 bar; 2 stops
8	Reburnish	80 → 3 km h <sup>-1</sup> ; 8 bar; 35 stops
9	Final effectiveness	50 → 3 km h <sup>-1</sup> ; 14 bar; 5 stops 100 → 3 km h <sup>-1</sup> ; 16 bar; 5 stops 160 → 3 km h <sup>-1</sup> ; 18 bar; 5 stops

the required technical specifications and was designed in line with the procedure of the SAE-J2430/BEEP (Brake Friction Products/Brake Effectiveness Evaluation Procedure). This procedure also simulates the parts of the Federal Motor Vehicle Safety Standards developed by the Brake Manufacturers Council of North America (BMC). The test procedure consists of instrument check stop, burnish, first effectiveness, fade, hot performance, cooling, recovery ramp, reburnish and final effectiveness. The detailed test conditions are described in the SAE-J2430 standard and are listed in table 3. Brake friction tests were performed on a single disc full-scale brake dynamometer. Each test was performed following the above sections in 312 braking cycles without any failure in the structural integrity for 14 h. During the dynamometer test, graphs were created by recording the braking effectiveness ( $\mu$ ), speed, pressure, torque and temperature values by using the data collection system. The dynamometer test was repeated three times under the same conditions for each disc and the mean values were taken.

## 2.5. Characterization techniques

The microstructures of the brake disc and coating powder were characterized with the scanning electron microscopy (SEM, JEOL-JSM 5910-LV) and x-ray diffraction (XRD, Bruker D8-Advanced). The elemental composition made in different areas from the cross-section and surfaces of the coating was obtained with an energy dispersive x-ray microanalysis (EDX, EX250) attached to the SEM. Microhardness measurements were performed using Vickers microhardness tester (Shimadzu HMV-2) for 15 s under a load of 300 g on the substrate disc and coating and the average hardness value was determined following 10 measurements for each sample. The wear amount of discs and linings was calculated by measuring the mass and thickness difference following the brake test. The surface roughness values were measured with the profilometer in the perpendicular direction to the sliding direction before and after the test and the average Ra value was determined.

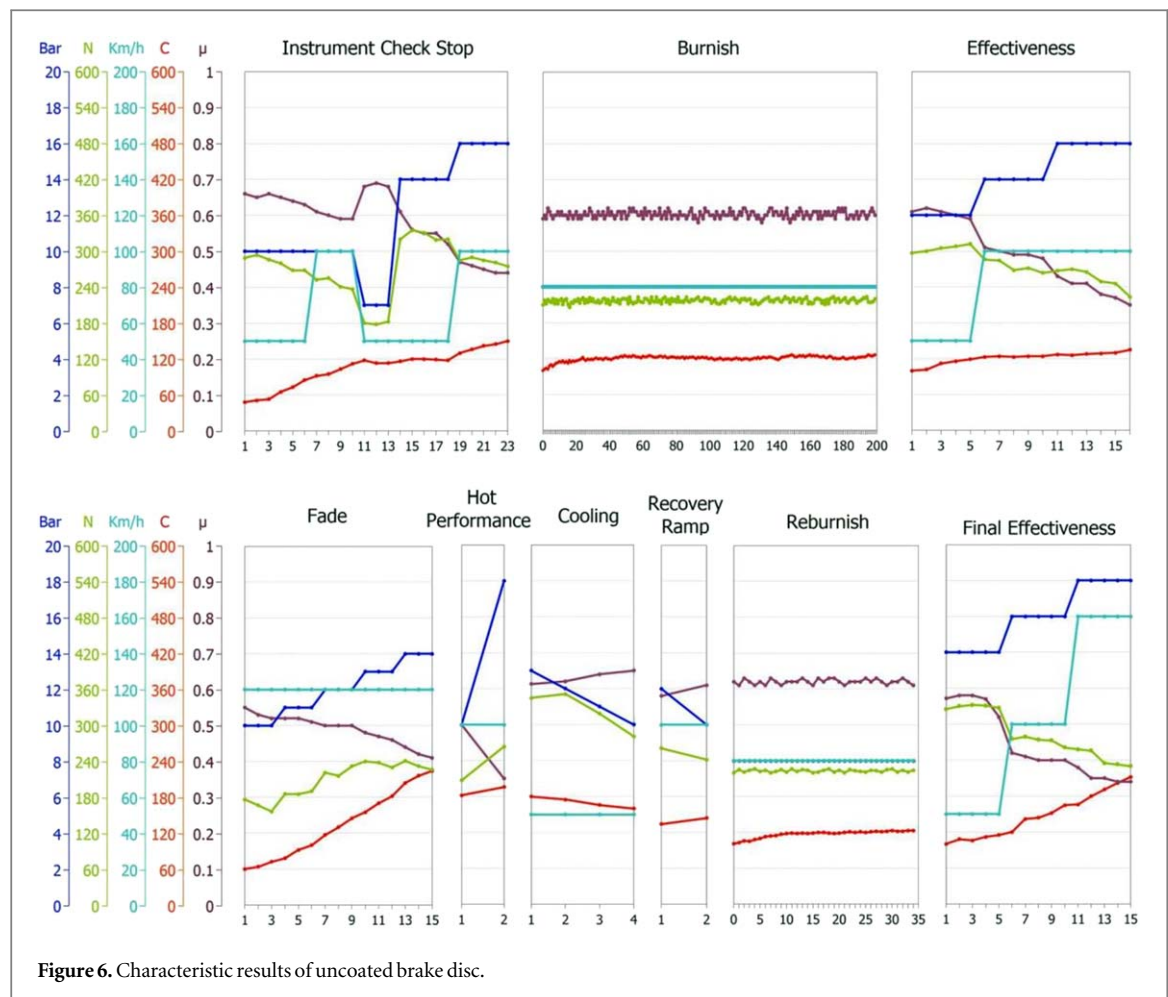


Figure 6. Characteristic results of uncoated brake disc.

### 3. Results and discussion

#### 3.1. Braking performance of discs

Brake performance tests of the 20NiCrBSi-WC12Co powder coated and uncoated discs were performed. Figures 6 and 7 shows the characteristic results obtained from the braking tests according to the SAE-J2430 procedure. Graphs were created by recording the coefficient of friction and temperature data which vary according to the normal force, contact pressure and speed. Mean values of varying parameters such as pressure, force, speed, temperature and coefficient of friction show the results of the test process starting with the instrument check stop and ending with the final effectiveness. The instrument check stop was designed to determine the appropriate dynamometer settings. In the burnish section, the disc-lining surfaces were acclimated to create a stable friction surface. In the burnish section, disc-lining surfaces were attuned to create a stable friction surface on the disc. Fluctuations were experienced in the coefficient of friction of the discs at the burnish section. This is explained by the coalescence and growth of roughness on the surface of the friction pairs. Repeated adhesion and release of the friction surfaces, causes an increase and decrease in the coefficient of friction [31]. In first effectiveness section, after application of five ramps at  $50 \text{ km h}^{-1}$  at  $100^\circ\text{C}$  and five additional ramps at  $100 \text{ km h}^{-1}$ , 6 brakings were performed under 16 bar pressure at the cold effectiveness section following the attuning stage. When the coefficient of friction changes of the discs were examined at this section, similar characteristics on the friction surface regarding the layer formation on the surface. However, the coated disc exhibited lower speed sensitivity figure 7. The coefficient of friction was found to have decreased while the contact temperature gradually increased. As the pressure increases, the coefficient of friction decreases as the actual contact area between the disc lining decreases [12]. The fade section is used to evaluate the effectiveness of the brake fading performance of the tested materials under high temperature. In this section, the coated disk exhibited a higher average coefficient of friction and a lower surface temperature than the uncoated one. The maximum surface temperature reached with the coated disc was  $201^\circ\text{C}$ , while the uncoated disc reached  $224^\circ\text{C}$ . At high temperatures, the coefficient of friction of both discs decreased compared to low-temperature values. This can be attributed to the formation of oxide or thermal film which protects the disc against mechanical wear at high temperatures. Here both brake discs exhibited significant fade resistance at high

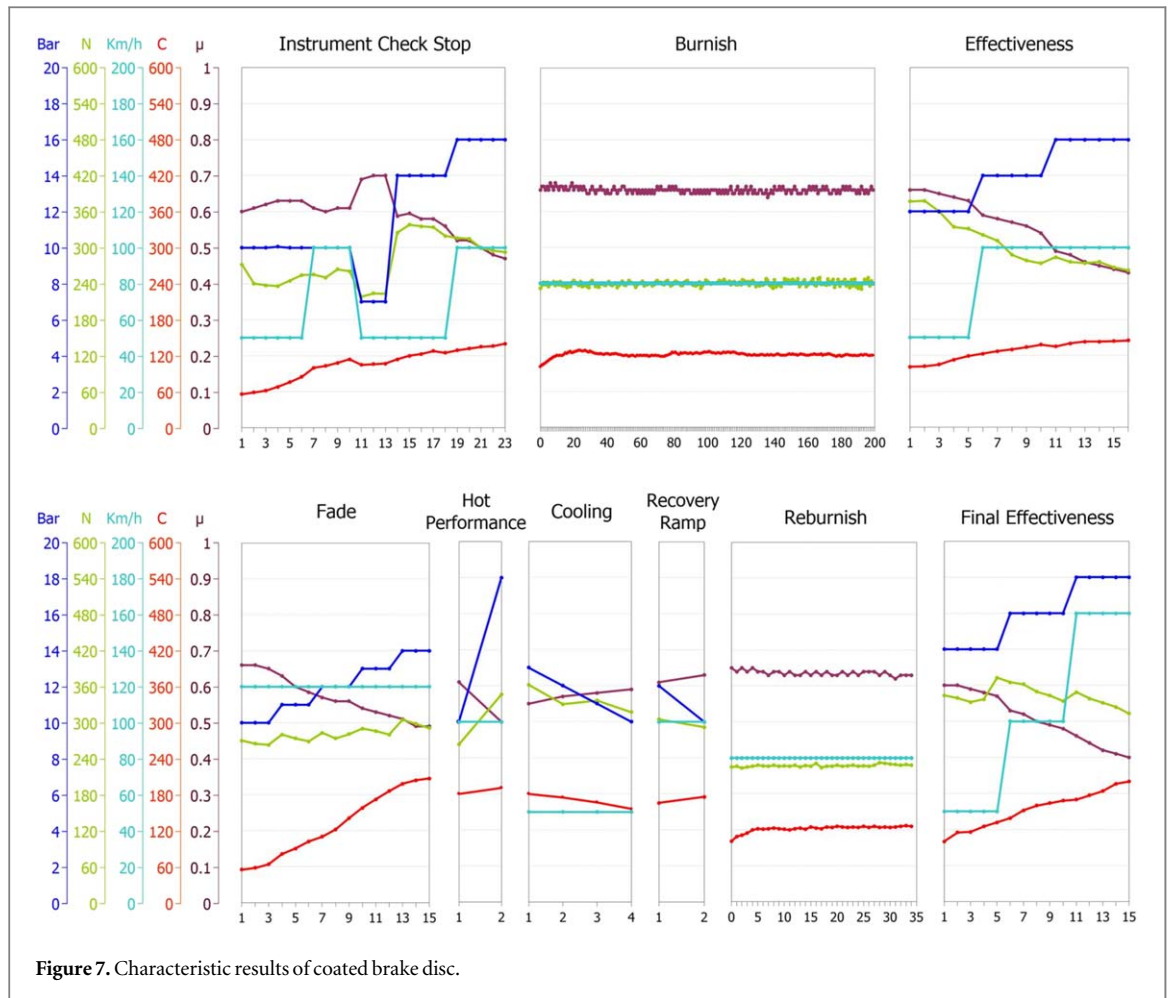


Figure 7. Characteristic results of coated brake disc.

temperatures. The fact that the amount of reduction in the friction efficiency of the coated disc at the braking pressure of 10 bar and 18 bar at a speed of  $100 \text{ km h}^{-1}$  is lower could be attributed to that there is balanced friction between the disc and the lining. In the cooling and recovery ramp sections, coefficient of friction of both discs increased. This indicates that the expected efficiency value was reached before the final effectiveness. Disc-lining surfaces are reburnish before high speeds are reached. The final effectiveness section reflects the speed sensitivity of the brakes up to  $160 \text{ km h}^{-1}$  vehicle speed. The final effectiveness of both discs decreased with the increase in speed. In the final effectiveness section, the uncoated disc was more sensitive to speed changes and dropped below  $\mu = 0.40$  at a speed of  $160 \text{ km h}^{-1}$  figure 6. At the end of the effectiveness sections, it is seen that the coated disc still has a very high coefficient of friction  $\mu = 0.40$  similarly to the uncoated disc's  $\mu = 0.35$ .

According to SAE-J2430, when evaluating the braking performance of the discs, the criteria such as check stop, first effectiveness, fade, hot performance and final effectiveness were taken into consideration for the same braking distance. At the end of the brake test effectiveness section, the coated disc exhibited comparable results to the original uncoated disc. The discs showed good fade resistance, low-speed sensitivity, good recovery capacity and relatively stable friction effectiveness. Throughout the test, the results obtained at the speeds of  $50 \text{ km h}^{-1}$ ,  $100 \text{ km h}^{-1}$  and  $160 \text{ km h}^{-1}$  and under variable pressures met the followed procedure criteria.

### 3.2. Friction and wear behavior

The amount of wear is shown in figure 8 as the average mass and thickness difference observed on the brake discs and linings after the dynamometer test. Here, the wear amount of the disc and the lining pair belonging to the disc are shown together. The mass loss of the brake lining of the coated disc was 3.69 g, the thickness loss of it was 2.327 mm, and the mass loss of the brake lining of the uncoated disc was 5.90 g, and the thickness loss of it was found to be 3.626 mm. The high temperature wear behavior of the brake pads depends largely on the material components. Degradation of the friction material at high temperatures is also associated with thermal decomposition of phenolic resins, which are often used as binders. The wear of the brake lining material can be related to the amount of released  $\text{CO}_2$ . The  $\text{CO}_2$  release corresponds to the wear, which is also expressed as mass loss of brake linings [32, 33]. Since the wear amount of the brake lining of the coated disc is lower, it could be said that the amount of  $\text{CO}_2$  emitted to the environment is lower.

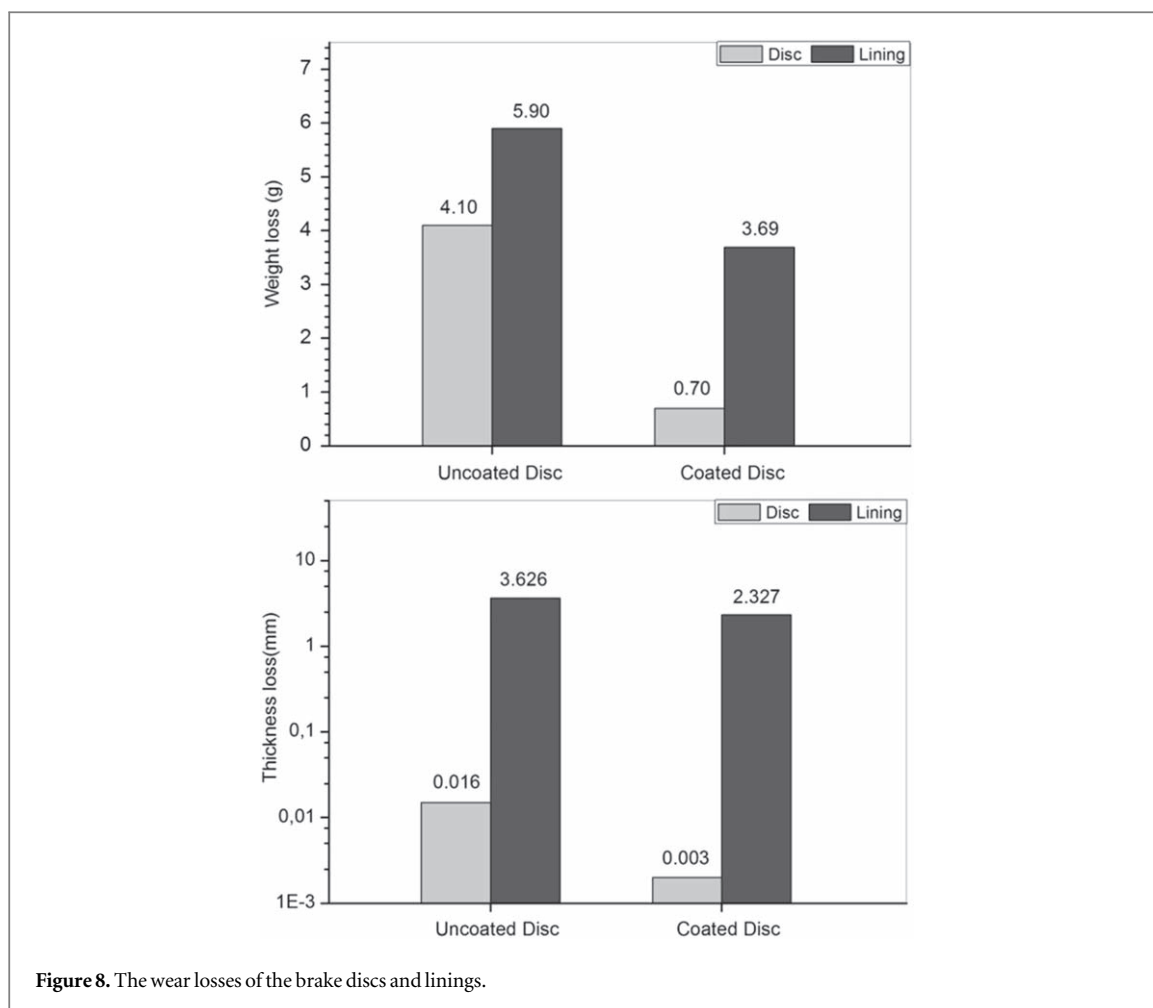


Figure 8. The wear losses of the brake discs and linings.

Table 4. Tribological results of uncoated and coated discs.

Characteristic	Uncoated Disc	Coated Disc
Hardness (HV <sub>0.3</sub> )	256 ± 15	928 ± 27
Weight loss of disc (g)	4.10	0.70
Weight loss of brake lining (g)	5.90	3.69
Thickness loss of disc (mm)	0.016	0.003
Thickness loss of brake lining (mm)	3.626	2.327
Roughness (Ra) of disc before test (μm)	1.737	0.922
Roughness (Ra) of disc after test (μm)	0.623	0.385
Roughness (Ra) of brake lining before test (μm)	2.121	2.130
Roughness (Ra) of brake lining after test (μm)	1.960	1.842
Average coefficient of friction (μ)	0.55	0.56
Highest surface temperature (°C)	224	201

In determining the efficiency of the friction of the pair in the brake system, the wear ratio is as important as the coefficient of friction. It is desirable that the coefficient of friction is high enough and that the wear rate is expected low [34]. Otherwise, the material consumption increases and thus the cost also increases. The high sliding wear resistance of the coatings is achieved by a combination of high microhardness and low porosity in the coating [35]. The coated disc 928 has a very high microhardness, such as HV<sub>0.3</sub>. The lower wear rate of the coated disc can be attributed to its high microhardness. The surface roughness is affected by the friction contact area. When the surface roughness changes, the contact will change and the wear performance will also be affected [36]. Uncoated brake disc with low hardness and high abrasion was found to have higher surface roughness values for disc lining pair at the end of the test. The coated disc having lower surface roughness produced a better friction layer. The coated disc has been exhibited good braking behavior with high surface hardness, low roughness. However, the braking effectiveness of the disc-lining pair is not only related to the differences in roughness. The difference in the chemical composition of the friction layers may also be responsible for the different levels of the friction.





**Figure 9.** Image of the worn surface after dynamometer tests of (a) uncoated disc, (b) coated disc.

After the completion of the test procedure, the values regarding wear, micro hardness, surface roughness and the average coefficient of friction of the discs and linings are summarized in table 4. The worn surfaces of the coated and uncoated discs after braking tests is shown in figure 9.

### 3.3. Microstructure and properties of frictional surfaces

XRD analysis of the coating powder and coating is shown in figure 10. The tungsten carbide WC phase was detected predominantly in the coating. The peak density of the WC phase can be attributed to the mass quantity of the WC12Co powder. It can also be suggested that B and Si contribute to the formation of carbide by increasing the viscosity because it is stated that it increases the viscosity of the coating powder by reducing the fusion temperature [37]. The spectrum of the coating shows the presence of carbide phases such as  $W_2C$ , and  $Cr_7C_3$ .  $Cr_7C_3$  (hexagonal) is a stable carbide and is effective in increasing the wear resistance of the coating.  $W_2C$  was not found in the raw material powder. Thus, during spraying, the primary carbides were converted into

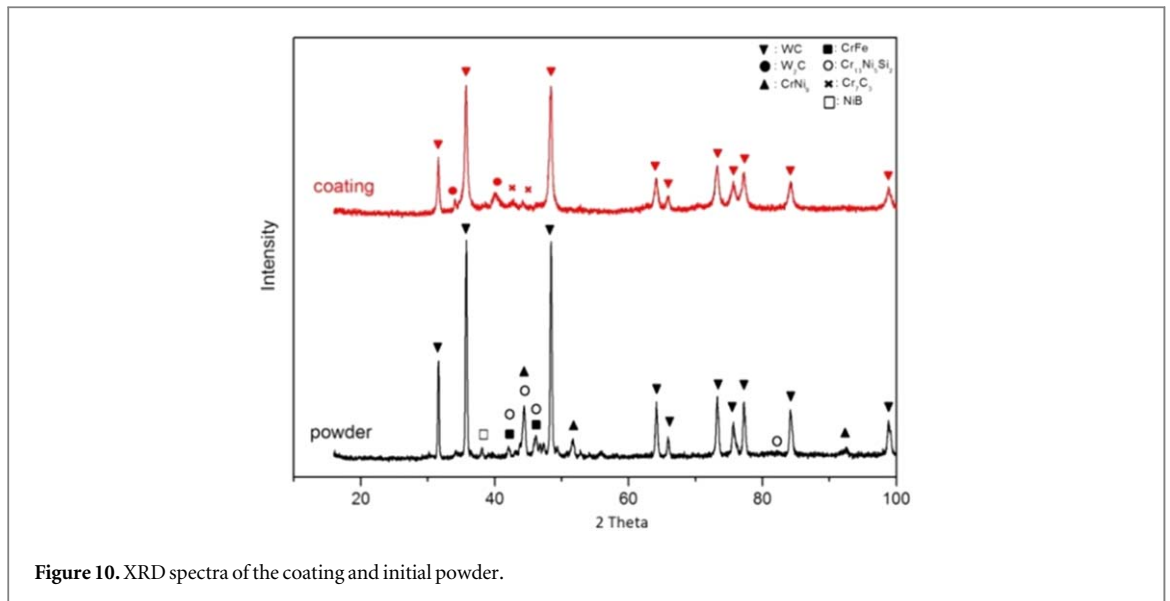


Figure 10. XRD spectra of the coating and initial powder.

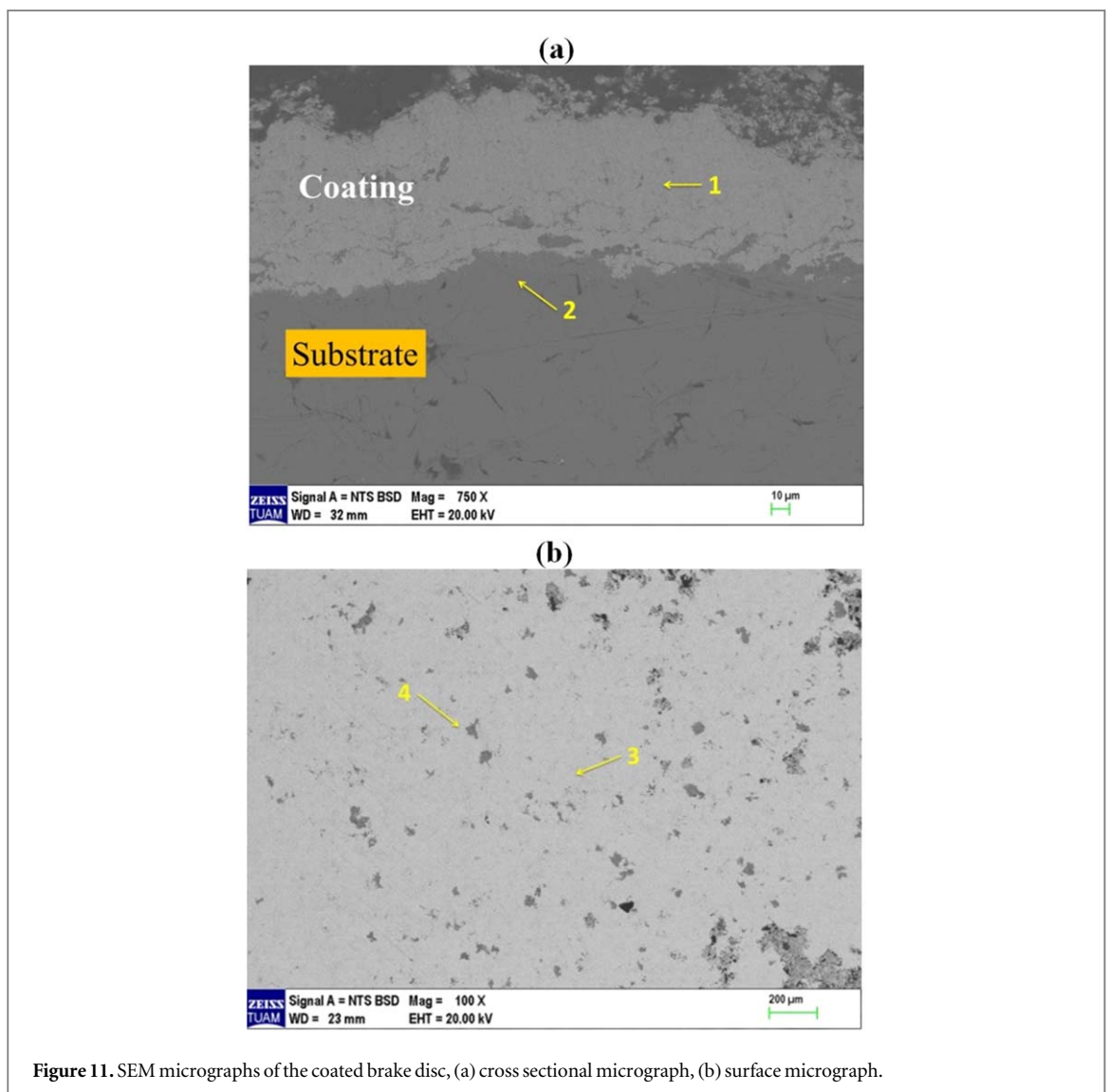
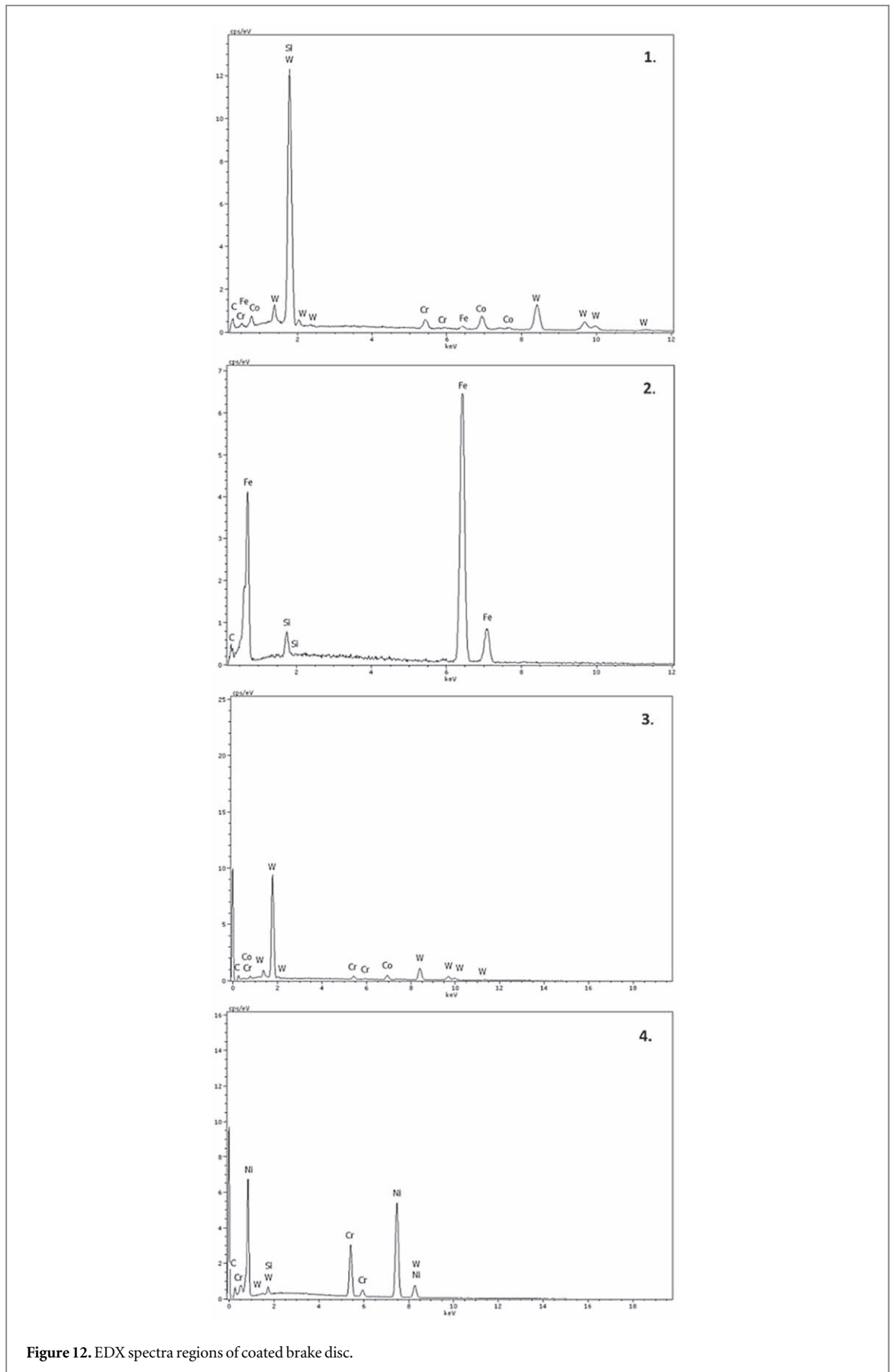
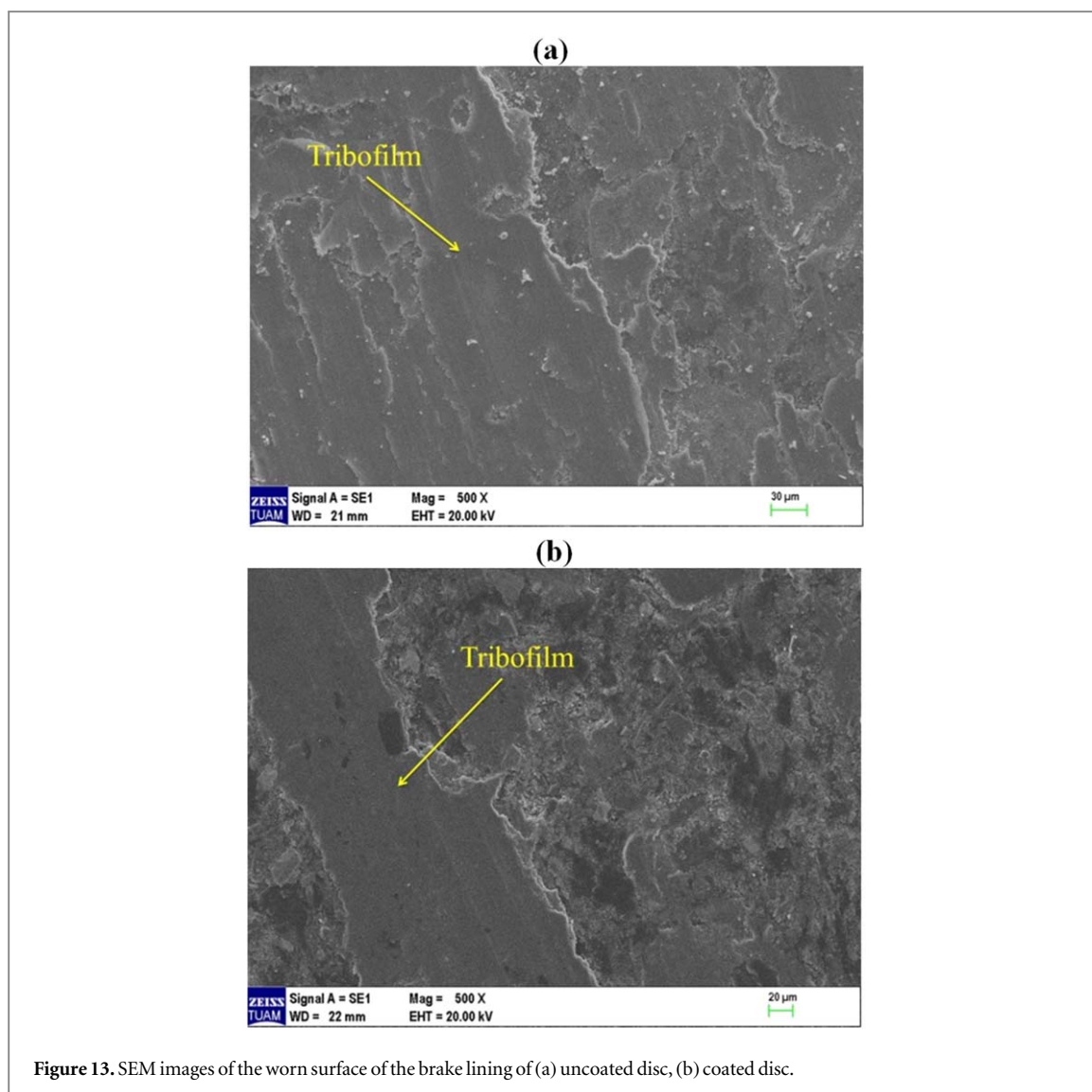


Figure 11. SEM micrographs of the coated brake disc, (a) cross sectional micrograph, (b) surface micrograph.

$W_2C$ . The presence of  $W_2C$  is generally attributed to limited decarburization that occurs during the HVOF process [38]. This formation depends on the accumulation conditions, the oxidizing atmosphere, the high cooling rates, and especially the high temperature. High microhardness is achieved by hard carbide phases in the



coating. In the HVOF technique, the amount of  $W_2C$  formed as a function of temperature and spray parameters was limited. This may be related to the high tendency of WC to dissolve in the matrix. Experimental results show that the WC phase is dispersed in the coating.



**Figure 13.** SEM images of the worn surface of the brake lining of (a) uncoated disc, (b) coated disc.

SEM micrographs of the cross-section and surface of a portion of the coating are shown in figure 11. The physical properties of the formed coating are summarized in table 4. Micrographs have shown that the coating has low porosity and lamella structure due to the high particle velocity of the HVOF system. With the precipitation of Ni element, a good metallurgical bond is formed between the coating and the substrate. Ni element, with excellent ductility and toughness, plays a dominant role in preventing the separation of carbide particles and is the main factor in increasing the wear resistance of the coating [39]. It also demonstrates that the coating is characterized by the absence of observable cracks on the surface.

The EDX spectra analyses in the numbered regions of the coating are shown in figure 12. In the analysis of the coating layer, zone 1 showed a microstructure rich in W and predominantly containing Co, Cr. The presence of the elements Fe and C in the coating layer shows that it diffused from the substrate to the coating by diffusion. In the analysis of zone 2, mainly Fe and Si were found in the cast iron substrate. In the analysis performed on the surface of the coating, it can be said that zone 3 contains W weighted Co, Cr and C elements. The presence of C, Cr and W elements in the Ni matrix was determined in zone 4.

The SEM micrograph of worn surfaces of the brake linings after the dynamometer test is shown in figure 13. Micro and macro friction layers are formed on the surface of the contact disk and lining pair due to the dry sliding. This friction layer is formed by the compression and interaction of the small wear residual particles. Its stability and character depend on the chemistry of the disc in contact, the interface temperature, the pressure and the sliding speed. The friction and wear behaviour of the linings is closely related to the worn surface of the brake disc with which they work [40]. The formation of the friction layer was observed on the surface of both linings.

A well-developed friction layer/plateau was not observed on the surface of the uncoated disc lining figure 13(a). A lot of craters are formed on this lining surface. The presence of the crater in the tribo-layer is

believed to be due to the fracture and breakdown of the laminated layer. Therefore, it could be said that the wear mechanism of the formed tribo-layer is not uniform. The worn surface of uncoated disc lining showed a rough surface topography with a lesser extent of secondary contact plateaus. This increased the amount of wear. It is obvious that the friction layer on the surfaces is discontinuous and does not always cover the entire friction surface. Wear rates depend on the ability to form and maintain constant friction layers/plateaus on the surface of the brake linings. On the contact surface of the coated disc lining, a more evident and more stable friction layer is seen to develop figure 13(b). On this lining surface, smooth secondary area plateaus and small amounts of wear residue were formed.

## 4. Conclusion

In this study, tribological behaviours such as friction and abrasion of 20NiCrBSi-WC12Co cermet coating accumulated on the brake disc by HVOF method were investigated. The coated and uncoated brake discs were tested on a full-scale brake dynamometer according to BEEP, and the obtained results were compared. The main findings can be summarized as follows:

HVOF cermet coating has a much higher microhardness and abrasion resistance compared to cast iron substrate with its combination of hard WC phase and mild Ni matrix. At the end of the test, the coated disc exhibited higher braking effectiveness than the uncoated disc. Throughout the test, the coated disc had lower speed sensitivity. Both brake discs tended to have low thermal fading. The brake lining of the coated disc was found to have a wear loss at a thickness of 2.327 mm, while the brake lining of the uncoated disc had a thickness loss of 3.626 mm. The coated disk revealed lower interface temperature with higher heat conduction. The Cermet coating was found to reduce abrasive wear on the brake disc surface, resulting in longer service life. Besides, it has been obtained that it also reduces the emission of particle matter to the environment with lower lining wear rate.

## ORCID iDs

Halil Kılıç  <https://orcid.org/0000-0001-6182-356X>

## References

- [1] Gultekin D, Uysal M, Aslan S, Alaf M, Guler M O and Akbulut H 2010 The effects of applied load on the coefficient of friction in Cu-MMC brake pad/Al-SiCp MMC brake disc system *Wear* **270** 73–82
- [2] Hinrichs R, Soares M R F, Lamb R G, Soares M R F and Vasconcellos M A Z 2011 Phase characterization of debris generated in brake pad coefficient of friction tests *Wear* **270** 515–9
- [3] Chandra Verma P, Menapace L, Bonfanti A, Ciudin R, Gialanella S and Straffelini G 2015 Braking pad-disc system: wear mechanisms and formation of wear fragments *Wear* **322–323** 251–8
- [4] Kılıç H, Mısırlı C and Mutlu I 2018 Investigating of braking and tribological features of granite powder additive brake linings *J. Balk. Tribol. Assoc.* **24** 52–63
- [5] Österle W and Urban I 2006 Third body formation on brake pads and rotors *Tribol. Int.* **39** 401–8
- [6] Timur M and Kılıç H 2013 Marble waste using produced of automotive brake pad of friction coefficient different pad brake pads with compresion *Pamukkale Univ. J. Eng. Sci.* **19** 10–4
- [7] Mutlu I, Eldogan O and Findik F 2005 Production of ceramic additive automotive brake lining and investigation of its braking characterisation *Ind. Lubr. Tribol.* **57** 84–92
- [8] Uyyuru R K, Surappa M K and Brusethaug S 2007 Tribological behavior of Al-Si-SiCp composites/automobile brake pad system under dry sliding conditions *Tribol. Int.* **40** 365–73
- [9] Eriksson M and Jacobson S 2000 Tribological surfaces of organic brake pads *Tribol. Int.* **33** 817–27
- [10] Chandra Verma P, Ciudin R, Bonfanti A, Aswath P, Straffelini G and Gialanella S 2016 Role of the friction layer in the high-temperature pin-on-disc study of a brake material *Wear* **346–347** 56–65
- [11] Bode K and Ostermeyer G-P 2014 A comprehensive approach for the simulation of heat and heat-induced phenomena in friction materials *Wear* **311** 47–56
- [12] Eriksson M, Bergman F and Jacobson S 2002 On the nature of tribological contact in automotive brakes *Wear* **252** 26–36
- [13] Sanders P G, Xu N, Dalka T M and Maricq M M 2003 Airborne brake wear bebris: size distributions, composition, and a comparison of dynamometer and vehicle tests *Environ. Sci. Technol.* **37** 4060–9
- [14] Kukutschová J, Roubíček V, Malachová K, Pavlíčková Z, Holuša R, Kubačková J, Mička V, MacCrimmon D and Filip P 2009 Wear mechanism in automotive brake materials, wear debris and its potential environmental impact *Wear* **267** 807–17
- [15] Mutlu I, Eldogan O and Findik F 2006 Tribological properties of some phenolic composites suggested for automotive brakes *Tribol. Int.* **39** 317–25
- [16] Wang Q, Chen Z H and Ding Z X 2009 Performance of abrasive wear of WC-12Co coatings sprayed by HVOF *Tribol. Int.* **42** 1046–51
- [17] Sari N Y and Yilmaz M 2008 Improvement of wear resistance of wire drawing rolls with Cr-Ni-B-Si + WC thermal spraying powders *Surf. Coatings Technol.* **202** 3136–41
- [18] Güney B and Mutlu İ 2019 Wear and corrosion resistance of Cr<sub>2</sub>O<sub>3</sub>-40%TiO<sub>2</sub> coating on gray cast-iron by plasma spray technique *Mater. Res. Express* **6** 96577

- [19] Federici M, Menapace C, Moscatelli A, Gialanella S and Straffelini G 2016 Effect of roughness on the wear behavior of HVOF coatings dry sliding against a friction material *Wear* **368–369** 326–34
- [20] Khosravifard A, Salahinejad E, Yaghtin A H, Araghi A and Akhbarizadeh A 2015 Tribochemical behavior of alumina coatings deposited by high-velocity oxy fuel spraying *Ceram. Int.* **41** 5713–20
- [21] Stoica V, Ahmed R, Itsukaichi T and Tobe S 2004 Sliding wear evaluation of hot isostatically pressed (HIPed) thermal spray cermet coatings *Wear* **257** 1103–24
- [22] Güney B, Mutlu I and Küçüksarıyıldız H 2019 The effect of flame spray coating on the tribological properties of brake disc *J. Polytech* (<https://dergipark.org.tr/tr/pub/politeknik/issue/33364/563277>) (<https://doi.org/10.2339/politeknik.563277>)
- [23] Huang S, Sun D, Xu D, Wang W and Xu H 2015 Microstructures and properties of NiCrBSi/WC biomimetic coatings prepared by plasma spray welding *J. Bionic Eng.* **12** 592–603
- [24] Stewart S, Ahmed R and Itsukaichi T 2004 Contact fatigue failure evaluation of post-treated WC-NiCrBSi functionally graded thermal spray coatings *Wear* **257** 962–83
- [25] Hidalgo V H, Varela F J B, Menéndez A C and Martínez S P 2001 A comparative study of high-temperature erosion wear of plasma-sprayed NiCrBSiFe and WC-NiCrBSiFe coatings under simulated coal-fired boiler conditions *Tribol. Int.* **34** 161–9
- [26] Miguel J M, Guilemany J M and Vizcaino S 2003 Tribological study of NiCrBSi coating obtained by different processes *Tribol. Int.* **36** 181–7
- [27] Ward L P and Pilkington A 2014 The dry sliding wear behavior of HVOF-sprayed WC: Metal composite coatings *J. Mater. Eng. Perform.* **23** 3266–78
- [28] Federici M, Menapace C, Moscatelli A, Gialanella S and Straffelini G 2017 Pin-on-disc study of a friction material dry sliding against HVOF coated discs at room temperature and 300 °C *Tribol. Int.* **115** 89–99
- [29] SAE J2430 1999 *Dynamometer Effectiveness Characterization Test for Passenger Car and Light Truck Brake Friction Products*, Surface Vehicle Standard (USA: Society of Automotive Engineers, Warrendale, Pennsylvania)
- [30] SAE J661 1997 *Brake Lining Quality Test Procedure* (USA: Society of Automotive Engineers, Warrendale, Pennsylvania)
- [31] Mutlu I, Oner C and Findik F 2007 Boric acid effect in phenolic composites on tribological properties in brake linings *Mater. Des.* **28** 480–7
- [32] Roubicek V, Raclavska H, Juchelkova D and Filip P 2008 Wear and environmental aspects of composite materials for automotive braking industry *Wear* **265** 167–75
- [33] Joo B S, Chang Y H, Seo H J and Jang H 2019 Effects of binder resin on tribological properties and particle emission of brake linings *Wear* **434–435** 202995
- [34] Güney B and Mutlu I 2019 Tribological properties of brake discs coated with Cr<sub>2</sub>O<sub>3</sub>-40% TiO<sub>2</sub> by plasma spraying *Surf. Rev. Lett.* **26** 1–12
- [35] Ang A S M, Howse H, Wade S A and Berndt C C 2016 Development of processing windows for HVOF carbide-based coatings *J. Therm. Spray Technol.* **25** 28–35
- [36] Güney B, Mutlu I and Gayretli A 2016 Investigation of braking performance of NiCrBSi coated brake discs by thermal spraying and melting *J. Balk. Tribol. Assoc.* **22** 331–46
- [37] Carrasquero E J, Lesage J, Puchi-Cabrera E S and Staia M H 2008 Fretting wear of HVOF Ni–Cr based alloy deposited on SAE 1045 steel *Surf. Coatings Technol.* **202** 4544–51
- [38] Zhang W C, Liu L B, Zhang M T, Huang G X, Liang J S, Li X and Zhang L G 2015 Comparison between WC-10Co-4Cr and Cr<sub>3</sub>C<sub>2</sub>-25NiCr coatings sprayed on H13 steel by HVOF *Trans. Nonferrous Met. Soc. China (English Ed.)* **25** 3700–7
- [39] Guo C, Zhou J, Chen J, Zhao J, Yu Y and Zhou H 2011 High temperature wear resistance of laser cladding NiCrBSi and NiCrBSi/WC-Ni composite coatings *Wear* **270** 492–8
- [40] Wang F and Liu Y 2014 Mechanical and tribological properties of ceramic-matrix friction materials with steel fiber and mullite fiber *Mater. Des.* **57** 449–55